NASA TECHNICAL MEMORANDUM

NASA TM X-52207

NASA TM X-52207

A REVIEW OF BALL MOTION IN AN ANGULAR CONTACT BALL BEARING

by R. J. Parker, E. V. Zaretsky, and W. J. Anderson
Lewis Research Center
Cleveland, Ohio

TECHNICAL PAPER proposed for presentation at Spring Lubrication Symposium sponsored by the American Society of Mechanical Engineers
New Orleans, Louisiana, June 6, 1966

NATIONAL AERONAUTICS AND SPACE ADMINISTRATION - WASHINGTON, D.C. - 1966

A REVIEW OF BALL MOTION IN AN ANGULAR CONTACT BALL BEARING

by R. J. Parker, E. V. Zaretsky, and W. J. Anderson

Lewis Research Center
Cleveland, Ohio

TECHNICAL PAPER proposed for presentation at

Spring Lubrication Symposium
sponsored by the American Society of Mechanical Engineers
New Orleans, Louisiana, June 6, 1966

NATIONAL AERONAUTICS AND SPACE ADMINISTRATION

A REVIEW OF BALL MOTION IN AN ANGULAR CONTACT BALL BEARING

by R. J. Parker, E. V. Zaretsky, and W. J. Anderson

Lewis Research Center
National Aeronautics and Space Administration
Cleveland, Ohio

E-3022

ABSTRACT

A significant portion of total ball-bearing friction results from friction due to sliding or spinning in the contacts of the balls and races. A brief review of the nature of this ball-race contact including analyses of ball spin and microslip and the factors contributing to the problem are presented in this paper.

NOMENCLATURE

A	contact area, sq in.
a_o	semi-major axis of contact ellipse, in.
b	semi-width of contact of two cylinders in contact, in.
b'	semi-width of no slip region of two cylinders in contact, in.
b_o	semi-minor axis of contact ellipse, in.
c	distance from center of contact area to center of no slip region, in.
d	ball diameter, in.
E	pitch diameter, in.
E_1, E_2	Young's modulus of elasticity, psi
E(k)	complete elliptic integral of the second kind
e,e',e"	surface displacements, in.
F	friction force, lbs
F_r	rolling resistance, lbs
f_k	coefficient of kinetic friction

f_s coefficient of spinning friction

K elastic constant

k modulus of complete elliptic integral of the second kind E(k)

M bearing torque due to spinning, lb-in.

M_s ball spinning moment, lb-in.

n number of balls

P_N normal load per unit length of two cylinders in contact, lb/in.

P_{No} normal ball load, lb

Q, Q', Q'' tangential traction, lb/in^2

Q_s frictional heat generation due to ball spinning on race, Btu/min

q tangential force per unit length of two cylinders in contact, lb/in.

R radius of ball or cylinder, in.

r' polar coordinate distance, in.

r_i limit of r integration, in.

S_{xy} compressive stress acting on any point on the contact area, psi

S_y compressive stress for two cylinders of unit length under rolling contact, psi

U peripheral velocity, in/min

V velocity, in/min

x,y,z distance in principal direction, in.

$\alpha_1, \alpha_2, \theta, \mu, \psi$ angles defined in figures 3 and 4, deg

β bearing contact angle, deg

β_i inner-race contact angle at load and speed, deg

β_o outer-race contact angle at load and speed, deg

γ rolling factor

δ Poisson's ratio

λ contact factor

ξ slip ratio for two cylinders in rolling contact

ξ_o slip ratio for ball rolling in conforming groove

ρ radius of groove, in.

φ polar coordinate angle, deg

ω angular velocity, rad/min

INTRODUCTION

The rolling contact phenomenon, the interaction of two or more bodies in rolling contact, has been the subject of much study, debate, and controversy for several decades. Many unresolved questions currently exist, in addition to numerous new problems which develop as machine elements become more complex and as loads, temperatures, and speeds increase within these elements.

In order to understand the various factors influencing rolling-element design, fatigue, and lubrication, an understanding of bearing kinematics is a prime prerequisite. While considerable analytical and experimental work have been conducted in this area, a summation under one cover at the time of this writing was nonexistent. Therefore, it is the objective of this article to treat rolling element kinematics in its most elementary comprehensive form. A review of the kinematics of rolling element bearings will be presented with specific emphasis on ball bearings under a thrust load. The effects on overall bearing friction losses of ball spinning and of rolling with microslip and elastic compliance will be discussed.

BALL MOTION IN AN ANGULAR CONTACT RACEWAY

Fatigue in bearings is a phenomenon dependent on element loading and rate of cycling. The rate of cycling is dependent on bearing geometry, the number of rolling elements, and the angular velocity of the inner race.

In figure 1 a section of an angular contact ball bearing under pure thrust load is shown. If ω_i is the angular velocity of the inner race, the velocity of point A is

$$V_A = \omega_i \overline{AB} \tag{1}$$

Similarly, if ω_o is the angular velocity of the outer race, then the velocity of point C is

$$V_C = \omega_o \overline{CD} \tag{2}$$

The velocity of the ball center V_o is

$$V_o = \frac{1}{2} (V_A + V_C) \tag{3}$$

Substituting equations (1) and (2) into equation (3) gives

$$V_o = \frac{1}{2} \left[\frac{\omega_i}{2} (E - d \cos \beta) + \frac{\omega_o}{2} (E + d \cos \beta) \right] \tag{4}$$

The angular velocity of the separator or cage and the ball set about the shaft axis is

$$\omega_o = \frac{V_o}{E/2} \tag{5}$$

Then

$$\omega_o = \frac{1}{2} \left[\omega_i \left(1 - \frac{d \cos \beta}{E} \right) + \omega_o \left(1 + \frac{d \cos \beta}{E} \right) \right] \tag{6}$$

The speed of the separator when the outer race is fixed is

$$\omega_c = \frac{\omega_i}{2}\left(1 - \frac{d \cos \beta}{E}\right) \tag{7}$$

Since $\beta < 90^o$, the separator speed is always less than half the shaft speed. When both races rotate, the speed of the inner race relative to the separator is

$$\omega_{i/c} = \omega_i - \omega_c = \frac{1}{2}(\omega_i - \omega_o)\left(1 + \frac{d \cos \beta}{E}\right) \tag{8}$$

The speed of the outer race relative to the separator is

$$\omega_{o/c} = \omega_o - \omega_c = \frac{1}{2}(\omega_o - \omega_i)\left(1 - \frac{d \cos \beta}{E}\right) \tag{9}$$

From equations (8) and (9), the speed of the inner race relative to the separator is always greater than that of the outer race relative to the separator; therefore, a point on the inner-race ball track will receive a greater number of stress cycles per unit time than will a point on the outer race.

For ball bearings that operate at nominal speeds under a thrust load, the centrifugal force on the balls is negligible and the forces that keep the ball in equilibrium are the two contact forces. For such conditions, the contact forces are equal and opposite, and the inner- and the outer-race contact angles are approximately equal.

The motion of a ball in angular contact ball bearings has been experimentally observed by Shevchenko [1] and by Hirano [2]. Shevchenko utilized high speed photography and Hirano measured the change in magnetic flux induced by a magnetized ball. Both means of observation were successful in determining the ball angular velocity and the axis of rotation of the balls. Results of these tests will be discussed later.

BALL SPIN

Spinning moment. - The previous section treated the velocities of bearing components in their most simplified form. In a thrust loaded ball bearing another velocity component, ball spin, is introduced. Ball spinning is responsible for a major portion of the overall friction in a thrust loaded bearing and can account for high heat generation rates [3]. Measurements of ball spinning friction have been performed by Reichenbach [3] and Miller [4] for various geometries and loads. Ball spinning moment in an angular contact ball bearing was determined by Poritsky, et al. [5] by integrating the friction force over the contact ellipse. Figure 2 illustrates the contact ellipse over which sliding due to spinning takes place. Since the sliding motion is a rotation about the ellipse center, the direction of sliding is normal to the radius vector to the point (x,y) as shown. The friction force is assumed to be in the direction opposite to that of sliding and of a magnitude proportional to the normal compressive force

$$dF = f_s S_{xy}\, dA \tag{10}$$

where f_s is the coefficient of spinning friction (assumed independent of the contact stress S_{xy}) and dA is the element of area. Introducing polar coordinates r, φ, the moment of the local friction force is seen to be

$$\begin{aligned} dM_s &= f_s S_{xy} r\, dA \\ &= f_s S_{xy} r^2\, dr\, d\varphi \end{aligned} \tag{11}$$

where S_{xy} is given by

$$S_{xy} = \frac{3P_{No}}{2\pi a_o b_o}\left[1 - \left(\frac{x}{a_o}\right)^2 - \left(\frac{y}{b_o}\right)^2\right]^{1/2} \tag{12}$$

Substituting from equation (12) into equation (11), and introducing r, φ, one obtains for the net moment

$$M_s = \frac{3f_s P_{No}}{2\pi a_o b_o}\int_0^{2\pi}\int_0^{r'} r^2\left\{1 - \left[\left(\frac{1}{a_o}\cos\varphi\right)^2 + \left(\frac{1}{b_o}\sin\varphi\right)^2\right]r^2\right\}^{1/2} dr\, d\varphi \tag{13}$$

where the limits of integration for r go from 0 to the edge of the ellipse

$$r' = \frac{a_o b_o}{\left[(b_o\cos\varphi)^2 + (a_o\sin\varphi)^2\right]^{1/2}} \tag{14}$$

The integration with respect to r may be carried out in terms of elementary functions. The φ-integration leads to a complete elliptic integral of the second order. Hence,

$$M_s = \frac{3}{8} f_s P_{No} a_o E(k) \tag{15}$$

where

$$k = \left[1 - \left(\frac{b_o}{a_o}\right)^2\right]^{1/2} \tag{16}$$

Ball spinning plus rolling will occur at one race contact, whereas rolling without spin will occur at the other even if the contact angle β is equal at both races. Rolling without spin will occur at the contact where the ball spinning moment is the greater. For the angular contact bearing illustrated in figure 1 having equal race curvatures, the semi-major axis of the contact ellipse will be greater at the inner race than at the outer race. Hence, the spinning moment will be greater

and rolling will occur at the inner race. At the outer race, spinning plus rolling will take place. This action is known as inner-race ball control.

Race curvature directly affects contact ellipticity. Thus, differences in race curvature at the inner and outer races will cause differences in spinning moments at the two race contacts and will govern where ball control takes place. Ball centrifugal force, which may be significant at high speeds, increases the load at the outer race, and ball control is generally shifted to the outer race.

In summation, if

$$M_{s_{(inner)}} > M_{s_{(outer)}}$$

then rolling will occur at the inner race while rolling with spinning will occur at the outer race. This phenomenon is referred to as inner race control. If, on the other hand

$$M_{s_{(inner)}} < M_{s_{(outer)}}$$

rolling will occur at the outer race while rolling with spinning will occur at the inner race. This is referred to as outer race control. The kinematics of a ball bearing is greatly affected by ball control.

Spin velocity. - Once the race where ball control occurs has been determined, the ball spin velocity can be calculated. Ball spin velocity is a function of the contact angle and the inner race speed. Figure 3(a) represents an angular contact ball bearing under thrust load with ball control at the outer race. From this figure,

$$V_B = \omega_i \left[\frac{E}{2} - \frac{d}{2} \cos \beta_i \right] \tag{17}$$

Solving for tan α_2,

$$\tan \alpha_2 = \frac{\overline{CO}}{\overline{OA}}$$

$$= \frac{\sin \beta_o}{\frac{E}{d} + \cos \beta_o} \tag{18}$$

From figure 3(a)

$$\mu = \frac{\pi}{2} + \beta_i - \beta_o + \alpha_2 \tag{19}$$

Solving for $\sin \alpha_1$,

$$\sin \alpha_1 = \frac{\overline{BD}}{\overline{BA}}$$

$$= \frac{\sin \mu}{\left\{1 + \left[\frac{E/d}{\sin (\beta_o - \alpha_2)}\right]^2 - 2\left[\frac{E/d}{\sin (\beta_o - \alpha_2)}\right]\cos \mu\right\}^{1/2}} \tag{20}$$

Solving for ω_{ball},

$$\omega_{ball} = \frac{V_B}{\overline{BH}}$$

$$= \frac{\omega_i[(E/d) - \cos \beta_i]}{(\sin \alpha_1 + \tan \alpha_2 \cos \alpha_1)} \tag{21}$$

$$\cdot \frac{1}{\left\{1 + \left[\frac{E/d}{\sin(\beta_o - \alpha_2)}\right]^2 - 2\left[\frac{E/d}{\sin(\beta_o - \alpha_2)}\right] \cos \mu\right\}^{1/2}}$$

Referring to figure 3(b) and solving for the velocity of the ball relative to the velocity of the inner race,

$$\bar{\omega}_{b/i} = \bar{\omega}_{ball} - \bar{\omega}_i \tag{22}$$

Solving for the angle ψ,

$$\psi = \beta_i - \beta_o + \alpha_2 \tag{23}$$

The angular velocity of the ball relative to the angular velocity of the inner race can be written

$$\bar{\omega}_{b/i} = \bar{\omega}_{ri} + \bar{\omega}_{si} \tag{24}$$

Solving for the spinning velocity at the inner race

$$\omega_{si} = \omega_{ball} \sin \psi + \omega_i \sin \beta_i$$

Substituting equations (21) and (23) into (25)

$$\omega_{si} = \left[\frac{\omega_i [(E/d) - \cos \beta_i]/(\sin \alpha_1 + \tan \alpha_2 \cos \alpha_1)}{\left\{ 1 + \left[\frac{E/d}{\sin(\beta_o - \alpha_2)} \right]^2 - 2 \left[\frac{E/d}{\sin(\beta_o - \alpha_2)} \right] \cos \mu \right\}^{1/2}} \right] \cdot \sin(\beta_i - \beta_o + \alpha_2) + \omega_i \sin \beta_i \tag{26}$$

For ball bearings that operate at nominal speeds, centrifugal forces are negligible and the contact angles at the inner- and outer-races remain essentially equal. Thus for outer race control, if $\beta_o = \beta_i$, equation (21) becomes

$$\omega_{ball} = \frac{\omega_i (E/d - \cos \beta_i)}{2 \cos \alpha_2} \tag{27}$$

and $\psi = \alpha_2$ and equation (25) becomes

$$\omega_{si} = \omega_{ball} \sin \alpha_2 + \omega_i \sin \beta_i \tag{28}$$

Substituting equation (27) into equation (28)

$$\omega_{si} = \frac{\omega_i (E/d - \cos \beta_i) \sin \alpha_2}{2 \cos \alpha_2} + \omega_i \sin \beta_i = \omega_i \left[\frac{\tan \alpha_2}{2} \left(\frac{E}{d} - \cos \beta_i \right) + \sin \beta_i \right] \tag{29}$$

Referring to figure 4(a), there is shown a similar bearing but with inner-race control. Comparing figure 4(a) with figure 3(a), it can readily be noted that the kinematics are different due to the fact that rolling occurs at the inner race contact. The solution to ω_{so} is similar to that of ω_{si}. Solving for the tangential velocity of the

ball at point B, V_B

$$V_B = \overline{BH}\omega_i$$

$$= \frac{\omega_i}{2}(E - d\cos\beta_i) \tag{30}$$

Solving for tan α_1,

$$\tan\alpha_1 = \frac{d/2}{\overline{AB}}$$

$$= \frac{\sin\beta_i}{E/d - \cos\beta_i} \tag{31}$$

Now assuming a cone rolling about line of zero velocity

$$\omega_{ball} = \frac{V_B}{\overline{BG}} \tag{32}$$

From figure 4(a)

$$\tan\alpha_1 = \frac{\overline{BD}}{\overline{AD}} \tag{33}$$

and

$$\tan\alpha_2 = \frac{\overline{DG}}{\overline{AD}}$$

Adding equations (33) and (34)

$$\tan\alpha_1 + \tan\alpha_2 = \frac{\overline{BD} + \overline{DG}}{\overline{AD}} = \frac{\overline{BG}}{\overline{AD}} \tag{35}$$

Substituting equation (35) into equation (32)

$$\omega_{ball} = \frac{V_B}{\overline{AD}(\tan\alpha_1 + \tan\alpha_2)} \tag{36}$$

$$= \frac{\omega_i \sin\beta_i}{(\tan\alpha_1 + \tan\alpha_2)\cos\alpha_1}$$

Solving for α_2; from figure 4(a)

$$\alpha_2 = \pi - \theta - \mu \tag{37}$$

and

$$\theta = \frac{\pi}{2} + \alpha_1 + \beta_i - \beta_o \tag{38}$$

Solving for μ ; from the law of cosines,

$$\overline{CA}^2 = \left(\frac{d}{2}\right)^2 + \overline{OA}^2 - 2\left(\frac{d}{2}\right)(\overline{OA})\cos\mu \tag{39}$$

$$\overline{OA}^2 = \left(\frac{d}{2}\right)^2 + \overline{CA}^2 - 2\left(\frac{d}{2}\right)(\overline{CA})\cos\theta \tag{40}$$

and from figure 4(a),

$$\overline{CA} = \frac{d}{2\sin\alpha_1} \tag{41}$$

Substituting equations (40) and (41) into equation (39), rearranging, and simplifying

$$\cos\mu = \frac{\left(\frac{d}{2}\right)^2 + \overline{OA}^2 - \overline{CA}^2}{2\left(\frac{d}{2}\right)(\overline{OA})} = \frac{\sin\alpha_1 - \cos\theta}{(\sin^2\alpha_1 + 1 - 2\cos\theta\sin\alpha_1)^{1/2}} \tag{42}$$

In order to solve for ω_{ball} determine the value of α_1 from equation (31) and determine the value of α_2 from equations (37), (38) and (42). Then ω_{ball} is obtained from equation (36).

Referring to figure 4(b), the spinning velocity at the inner race is

$$\omega_{so} = \omega_{ball}\sin(\beta_i + \alpha_1 - \beta_o) \tag{43}$$

For the special case where the contact angles β_i and β_o are equal, the spinning velocity at the outer race for inner race control is given by

$$\omega_{so} = \omega_{ball} \sin \alpha_1 \tag{44}$$

The effects on bearing operation of ball spin can be seen once the spinning moment, spinning velocity, and the location of race control have been determined.

The heat developed in the ball-race contacts due to spinning is given by

$$Q_s \propto n\omega_s M_s \tag{45}$$

The bearing torque due to spinning is then given by

$$M = \frac{Q_s}{\omega_i} \tag{46}$$

The frictional heat generated at the ball-race contact where spinning takes place accounts for a significant portion of the total bearing friction loss. Where centrifugal forces are significant, the normal load at the outer race-ball contact is increased and the resulting divergence of contact angles tends to increase the spinning velocity, and aggravate the problem of heat generation.

The effects of ball spinning can be minimized by decreasing the size or mass of the balls, using more open race curvatures, and by using smaller contact angles. Care must be taken in adjusting the latter two design features since the resulting increase in stress could produce a significant decrease in fatigue life.

The heat generation in the ball-race contacts can cause thermal gradients in the bearing which induce thermal stresses which in turn may affect fatigue life. In addition, this heat generation must be minimized for bearings used in cryogenic or other marginal lubrication applications as shown by Scibbe and Anderson [8].

Another factor that may further complicate the analysis of motion in a ball bearing under thrust load is the gyroscopic moment that acts on each ball. This gyroscopic moment, which may be great enough to cause slip at the ball-race contact in high-speed lightly-loaded bearings with large balls, results in a skewed direction of the rolling axis so that ω_{ball} does not lie in the x-z plane of figure 3. Hirano in reference [2] has shown that consideration of this gyroscopic moment was necessary to explain his experimental results with the theoretical works of Jones [7].

SLIP AND ELASTIC COMPLIANCE OF BODIES IN CONTACT

True rolling, in which no relative slip of the contacting surfaces of two bodies under a normal compressive load occurs, is for all practical purposes nonexistent. For true rolling to occur, (a) the contacting materials must be perfectly inelastic or (b) the local tangential friction force developed in the contact area must equal or exceed the force necessary to cause local tangential elastic deformation and prevent interfacial slip. The latter phenomenon is known as elastic compliance.

The solution of slip within the contact region has been summarized and discussed by Johnson [9]. Carter [10] presented the solution to the two-dimensional problem and, subsequently, Poritsky [11] discussed the problem in more detail.

Referring to figure 5, there is shown two cylinders of unit length of radii R_1 and R_2 in rolling contact at peripheral velocities U_1 and U_2 under a normal force P_N producing a Hertzian contact of width 2b with a stress distribution of S_y. A tangential force q due to kinetic friction f_k is present without sliding where $q < f_k P_N$. (Slip is to be differentiated from slide as follows: slip refers to a relative velocity at a point in the contact area, whereas slide refers to overall body movement associated with slip at all points in the contact area.)

Where complete slip is present in the contact area, at a specific value of y on the contact area the tangential traction is

$$Q' = f_k S_y = \frac{2 f_k P_N}{\pi b}\left(1 - \frac{y^2}{b^2}\right)^{1/2} \tag{47}$$

The traction produces surface strains in the contact area given by

$$\frac{\partial e'}{\partial y} = - \frac{4 f_k P_N K y}{b^2} \tag{48}$$

where the elastic constant

$$K = \frac{1 - \delta_1^2}{\pi E_1} \tag{49}$$

To obtain a region of no-slip a second tangential traction given by

$$Q'' = - \left(\frac{b'}{b}\right)^2 \frac{2 f_k P_N}{\pi b}\left[1 - \frac{(y + c)^2}{b^2}\right]^{1/2} \tag{50}$$

acting over the strip of width 2b' (the no slip region) is added to Q', equation (47), to give a value Q. The strains due to Q", by

analogy with equation (48), are given by

$$\frac{\partial e''}{\partial y} = \left(\frac{b'}{b}\right)^2 \frac{4f_k P_N (y + c)K}{b'^2}$$

$$= \frac{4f_k P_N (y + c)K}{b^2} \tag{51}$$

These distributions of traction and strain are illustrated in figure 6(a). Thus the net strain in the no slip region is

$$\frac{\partial e}{\partial y} = \frac{\partial e'}{\partial y} + \frac{\partial e''}{\partial y}$$

$$= \frac{4f_k P_N Kc}{b^2} = \text{constant} \tag{52}$$

Applying equation (52) to each body in turn and remembering that the traction on the lower surface is opposite in sign to that on the upper surface gives a slip ratio

$$-\xi = \frac{\Delta U}{U} = \frac{2(U_1 - U_2)}{(U_1 + U_2)} = \frac{\partial e_1}{\partial y} - \frac{\partial e_2}{\partial y}$$

$$= \frac{4f_k P_N (K_1 + K_2)c}{b^2} = \text{constant} \tag{53}$$

The value of b' is determined by the equilibrium of the integrated traction Q with the applied force q, resulting in

$$\frac{b'}{b} = \left(1 - \frac{q}{f_k P_N}\right)^{1/2} \tag{54}$$

In figure 6(a), for rolling contact

$$c = b - b' \tag{55}$$

Where the bodies are stationary, the center of no slip or locked region coincides with the center of the contact area as shown in figure 6(b), therefore $c = 0$.

Solving for c in equation (55) in accordance with equation (54) the expression for the slip ratio between two cylinders equation (53) becomes

$$\xi = -\frac{4f_k P_N (K_1 + K_2)}{b}\left[1 - \left(1 - \frac{q}{f_k P_N}\right)^{1/2}\right] \tag{56}$$

The case of a ball rolling on a grooved surface is somewhat different than a cylinder or roller in rolling contact with another roller or a plane surface. As shown in figure 7, the ball rolls about the X - X' axis and makes contact with the grooved surface from points 1 to 4. If the groove is fixed, then for zero slip over the contact ellipse no point within the ellipse should have a velocity in the direction of rolling. The surface of the contact ellipse is curved, however, so that the points 1 and 4 are at different radii from the X - X' axis than are points 2 and 3. For an inelastic ball, points 1 and 4 must have different velocities with respect to the X - X' axis than do points 2 and 3 because the velocity of any point on the ball relative to the X - X' axis equals the angular velocity times the radius from the X - X' axis. Slip must occur at various points over the contact ellipse unless the body is so elastic that yielding can take place in the contact area to prevent interfacial slip. The theory of Reynolds [12] and

later Heathcote [13] assumed that the interfacial slip took place, and that the forces required to make a ball roll are the forces required to overcome the friction due to interfacial slip. In the contact ellipse, according to Heathcote's theory, rolling without slip will occur at a specific radius from the X - X' axis. Where the radius is greater than this radius to the rolling point, slip will occur in one direction, and, where it is less than the radius to this rolling point, slip will occur in the other direction. In figure 7(b) the lines to points 2 and 3 represent the approximate location of the rolling bands, and the arrows shown in the three portions of the contact area represent the directions of interfacial slip when the ball is rolling out of the page.

The location of the two rolling bands relative to the axis of the contact ellipse can be obtained by means of a summation of the forces acting on the ball in the direction of rolling.

This problem was solved by Anderson [14], Halling [15], and Johnson [9]. The solution that follows is that of Johnson [9].

Referring again to figure 7, the ball of radius R rolls in a closely conforming groove of radius ρ. A normal load P_{N_o} produces an elliptical contact area having semi-major and semi-minor axes a_o and b_o respectively (fig. 8) which, it will be assumed, are given with sufficient accuracy by the Hertz theory.

From the Hertzian equations [16 and 17],

$$b_o^2 = \frac{3P_{N_o}(K_1 + K_2)R}{2\lambda a_o} \tag{57}$$

where

$$\lambda = \left[\frac{1 - \frac{R}{2\rho}}{E(k)}\right] \tag{58}$$

$$\left.\begin{aligned} K_1 &= \frac{1 - \delta_1^2}{\pi E_1} \\ K_2 &= \frac{1 - \delta_2^2}{\pi E_2} \end{aligned}\right\} \tag{59}$$

and $E(k)$ is the complete elliptic integral of the second kind. The compressive stress S_{xy}, acting at any point is as follows [17]

$$S_{xy} = \frac{3P_{N_o}}{2\pi a_o b_o}\left[1 - \left(\frac{x}{a_o}\right)^2 - \left(\frac{y}{b_o}\right)^2\right]^{1/2} \tag{60}$$

Assuming that the transverse profile of the ball can be specified by

$$z \approx \frac{x^2}{2R} \tag{61}$$

the peripheral velocity of points on the surface of the ball is given by

$$U_1 = \omega\left(R - \frac{x^2}{2R}\right) \tag{62}$$

while points on the groove move with a constant velocity U_2. Heathcote [13] maintained that rolling without sliding would take place on two bands, symmetrically disposed about the center line of the contact ellipse. However, as previously discussed, this conclusion takes no account of the ability of the surfaces to deform elastically and accomodate the difference in velocity by an extension of one surface and a compression of the other.

Johnson [9] analyzes the problem of tangential elastic compliance by dividing the elliptical contact area into thin slices parallel to the rolling direction and then applying the two-dimensional Carter-Poritsky theory to individual slices, neglecting any interaction between them. This approach is expected to be valid where the contact ellipse is narrow in the direction of rolling.

Referring to figure 8, consider a strip at a distance x from the center line, then by equations (53) and (62)

$$\xi = \frac{U_1 - U_2}{\omega R} = 1 - \frac{U_2}{\omega R} - \frac{x^2}{2R^2}$$

$$= \xi_o - \frac{x^2}{2R^2} \tag{63}$$

where ξ is the slip ratio for the strip and ξ_o is the slip ratio for the overall motion of the ball.

To apply the solution for two cylinders in contact to each individual strip, substitute equation (53) into (63). Then

$$\frac{4f_k P_N (K_1 + K_2)c}{b^2} = \xi_o - \frac{x^2}{2R^2} \tag{64}$$

where the semi-length of the strip

$$b = b_o\left[1 - \left(\frac{x}{a_o}\right)^2\right]^{1/2} \tag{65}$$

and where P_N is the intensity of load per unit length on the strip. Solving for P_N

$$P_N = \frac{3P_{N_o} b^2}{4b_o^2 a_o} = \frac{\lambda b^2}{2R(K_1 + K_2)} \tag{66}$$

from Hertzian equations and equations (57) and (60).

Substituting equation (66) into equation (64) and rearranging gives

$$\frac{c}{b} = \frac{2R}{4f_k \lambda b}\left(\xi_o - \frac{x^2}{2R^2}\right) \tag{67}$$

Multiplying equation (67) by Ra_o^2/Ra_o^2 and combining terms gives

$$\frac{c}{b} = \frac{a_o^2}{4f_k R\lambda b}\left[\left(\frac{2R^2\xi_o}{a_o^2}\right) - \left(\frac{x}{a_o}\right)^2\right] \tag{68}$$

Let

$$\gamma^2 = \frac{2R^2\xi_o}{a_o^2} \tag{69}$$

Then

$$\frac{c}{b} = \frac{a_o^2}{4f_k R\lambda b}\left[\gamma^2 - \left(\frac{x}{a_o}\right)^2\right] \tag{70}$$

It follows from the theory of two rollers in contact, some slip will occur at the trailing end of the elemental strip for which the slip ratio ξ is not zero. Equation (70) defines the amount of slip at any value of x. There will be no slip where c is zero. At this value of c, $x = \pm \gamma a_o$. At other values of x some slip occurs. (c/b cannot exceed unity, which corresponds to complete slip of the strip.)

The tangential force per unit length transmitted by each strip is found from equations (54) and (55) where

$$\frac{q}{f_k P_N} = 1 - \left(\frac{b'}{b}\right)^2 = \frac{c}{b}\left(2 - \frac{c}{b}\right) \tag{71}$$

Using equation (66)

$$q = \left(\frac{3f_k P_{N_o}}{4a_o}\right)\left(\frac{b}{b_o}\right)^2\left(\frac{c}{b}\right)\left[2 - \left(\frac{c}{b}\right)\right] \tag{72}$$

q is of opposite sign inside and outside the no-slip bands. For the ball to be in equilibrium when rolling freely in a straight groove there must be no resultant couple about an axis through the center of the ball. Therefore,

$$\int_0^{a_o} q(R - z)\, dx = \int_0^{a_o} q\left(R - \frac{x^2}{2R}\right) dx = 0 \tag{73}$$

This condition determines the value of γ and hence the position of the no-slip bands.

The resistance to rolling is then given by

$$F_r = 2 \int_0^{a_o} q \cdot dx \tag{74}$$

Equations (70), (72), (73), and (74) provide a complete solution to the tangential tractions, microslip and rolling resistance due to slip in any particular situation.

It follows from the analysis that when the coefficient of friction is so high that slip is restricted to a vanishingly small region at the trailing edge of the contact ellipse, $\gamma = 0.5$, that is, the no-slip lines are located at $x = \pm 0.5\, a_o$. For the Heathcote assumption of sliding at all points within the contact ellipse except on the no-slip lines, $\gamma \approx 0.35$. From the Heathcote assumption the rolling resistance is

$$F_r = \frac{0.080\, f_k P N_o a_o^2}{R^2} \tag{75}$$

To determine γ for a given application, a value of γ lying between the extreme values of 0.35 and 0.5 is assumed. Then equation (70) gives the amount of slip on each strip. Substituting equations (70) and (72) into equation (73) provides a check on whether the value of γ which has been chosen is correct. Having obtained a value of γ which satisfies equation (73), the rolling resistance can be found from equation (74). Referring to figure 9, Johnson [9] calculated the amount of microslip on the contact ellipse for two conditions presented in table I for a steel ball rolling freely in a conforming groove. For case (a) (fig. 9(a)) slip occurs over a substantial portion of the contact area. Whereas, for case (b) figure 9(b), the slip is more moderate over the contact area, occurring at the trailing end. Johnson [9] has experimentally observed microslip areas similar to those in figure 9.

The effects of rolling with spin were treated by Johnson in [9], [18], and [19] and by Halling in [15] and [20]. Johnson has reported that the spinning moments are less for rolling with spinning than for spinning alone. He has also shown experimentally that locked regions (elastic compliance) do occur to various extents depending on friction coefficient, spinning velocity, and rolling velocity.

In the analysis of roller and ball, there was no consideration of the effect of lubricant in the contact area. If a lubricant film is present, there are several questions which arise. Among these are, can there be regions of elastic compliance or no-slip (locked) regions as are illustrated in figures 7 and 9? If such regions exist, are they modified by the presence of a lubricant film? While no theoretical or experimental work considering the presence of a lubricant is reported

in the literature, it is interesting to speculate as to the effect.

An elastohydrodynamic film can change both the stress distribution and contact geometry for two rolling bodies in contact. Additionally, standard lubricants may become pseudosolids under high rolling-contact pressure. If this be so, the lubricant may be capable of transmitting the shear stresses which are necessary to maintain elastic compliance. If, however, the lubricant does not act as a pseudosolid the probable condition existing would be that approaching the assumptions of Heathcote [13] and, for a ball in a groove, $\gamma \rightarrow 0.35$.

As of the date of this writing both theoretical and experimental work need to be performed in this area to determine the effect of a lubricant on elastic compliance, to determine the effect of elastic compliance on contact stresses; and to determine if a relation exists between elastic compliance and rolling-element fatigue.

REFERENCES

1. R. P. Shevchenko and P. Bolan, "A Visual Study of Ball Motion in a High-Speed Thrust Bearing," SAE Paper 37 presented at the Annual Meeting, January 14-18, 1957.

2. F. Hirano, "Motion of a Ball in Angular-Contact Ball Bearing," ASLE Trans., vol. 8, no. 4, October, 1965, pp. 425-434.

3. G. S. Reichenbach, "The Importance of Spinning Friction in Thrust-Carrying Ball Bearings," J. Basic Eng., vol. 82, no. 2, June, 1960, pp. 295-301.

4. S. T. Miller, R. J. Parker and E. V. Zaretsky, "Apparatus for Studying Spinning Friction," NASA Tech. Note D-2796, May, 1965.

5. H. Poritsky, C. W. Hewlett, Jr. and R. E. Coleman, Jr., "Sliding Friction of Ball Bearings of the Pivot Type," J. Appl. Mech., vol. 14, no. 4, December, 1947, pp. 261-268.

6. A. B. Jones, "The Life of High-Speed Ball Bearings," ASME Trans. vol. 74, no. 5, July, 1952, pp. 695-703.

7. A. B. Jones, "Ball Motion and Sliding Friction in Ball Bearings," J. Basic Eng., vol. 81, no. 1, March, 1959, pp. 1-12.

8. H. W. Scibbe and W. J. Anderson, "Evaluation of Ball-Bearing Performance in Liquid Hydrogen at DN Values to 1.6 Million," ASLE Trans., vol. 5, no. 1, 1962, pp. 220-232.

9. K. L. Johnson, "Tangential Tranctions and Micro-slip in Rolling Contact," Rolling Contact Phenomena, J. B. Bidwell, ed., Elsevier Pub. Co., 1962, pp. 6-28.

10. F. W. Carter, "On the Action of a Locomotive Driving Wheel," Roy. Soc. Proc., ser. A, vol. 112, 1926, pp. 151-157.

11. H. Poritsky, "Stresses and Deflections of Cylindrical Bodies in Contact with Application to Contact of Gears and of Locomotive Wheels," J. Appl. Mech., vol. 17, no. 2, June, 1950, pp. 191-201.

12. O. Reynolds, "On Rolling Friction," Phil. Trans. Roy. Soc. (London), vol. 166, 1876, pp. 155-174.

13. H. L. Heathcote, "The Ball Bearing in the Making, Under Test and in Service," Proc. Inst. Automotive Eng., vol. 15, 1921, pp. 569-702.

14. E. E. Bisson and W. J. Anderson, "Advanced Bearing Technology, NASA SP-38, 1964, pp. 145-149.

15. J. Halling, "Microslip Between a Rolling Element and Its Track Arising from Geometric Conformity and Applied Surface Tractions," J. Mech. Eng. Sci., vol. 6, no. 1, March, 1964, pp. 64-73.

16. H. Hertz, Gesammelte Werke, vol. 1, (Leipzig) 1895, English Translation in "Miscellaneous Papers," H. Hertz, 1896.

17. A. B. Jones, New Departure-Analysis of Stresses and Deflections, vols. I and II, New Departure Div., General Motors Corp., 1946.

18. K. L. Johnson, "A Note on the Influence of Elastic Compliance on Sliding Friction in Ball Bearings," J. Basic Eng., vol. 82, no. 4, December, 1960, pp. 889-890.

19. K. L. Johnson, "The Influence of Elastic Deformation Upon the Motion of a Ball Rolling Between Two Surfaces," Inst. Mech. Engrs. Proc., vol. 173, no. 34, 1959, pp. 795-810.

20. J. Halling, "The Microslip Between a Ball and Its Track in Ball-Thrust Bearings," J. Basic Eng., vol. 88, no. 1, March, 1966, pp. 213-220.

TABLE I. - EXAMPLES OF BALL ROLLING IN A CONFORMING GROOVE (ref. 9)

Example	(a) (Fig. 9(a))	(b) (Fig. 9(b))
Ball Radius/Groove Radius (R/p)	0.948	0.815
Contact Ellipticity (a_o/b_o)	6.9	3.1
Contact Size/Ball Radius (a_o/R)	0.103	0.066
$\frac{\text{Rolling Resistance}}{\text{Normal Load}}$, F_r/P_{N_o} :		
Johnson's Theory	7.0×10^{-5}	1.9×10^{-5}
Heathcote's Theory	8.5×10^{-5}	3.4×10^{-5}

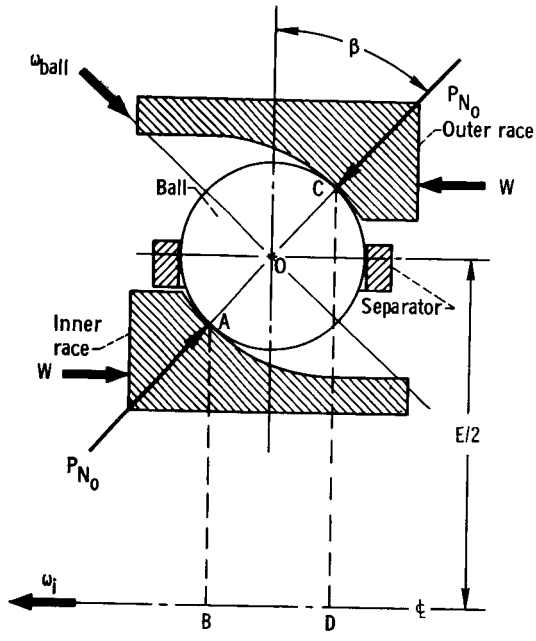

Figure 1. - Ball in an angular-contact raceway.

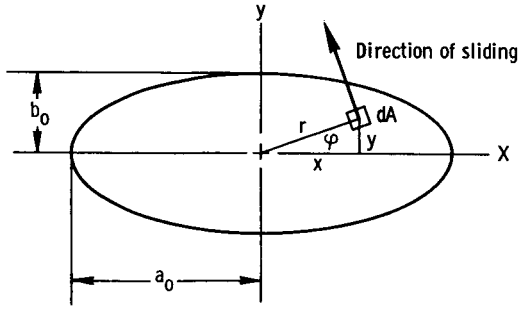

Figure 2. - Contact ellipse (ref. 5).

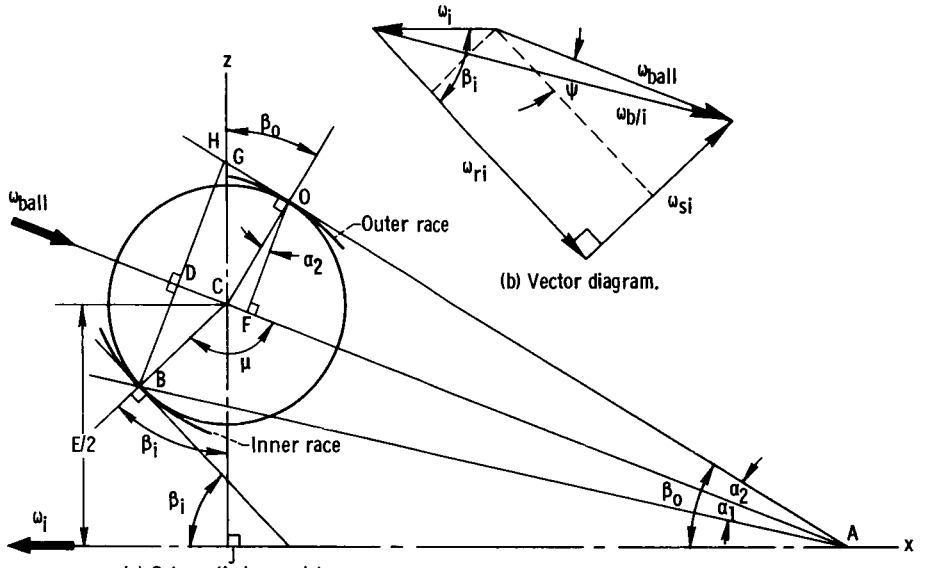

(b) Vector diagram.

(a) Schematic (no scale).

Figure 3. - Outer race control (ref. 8).

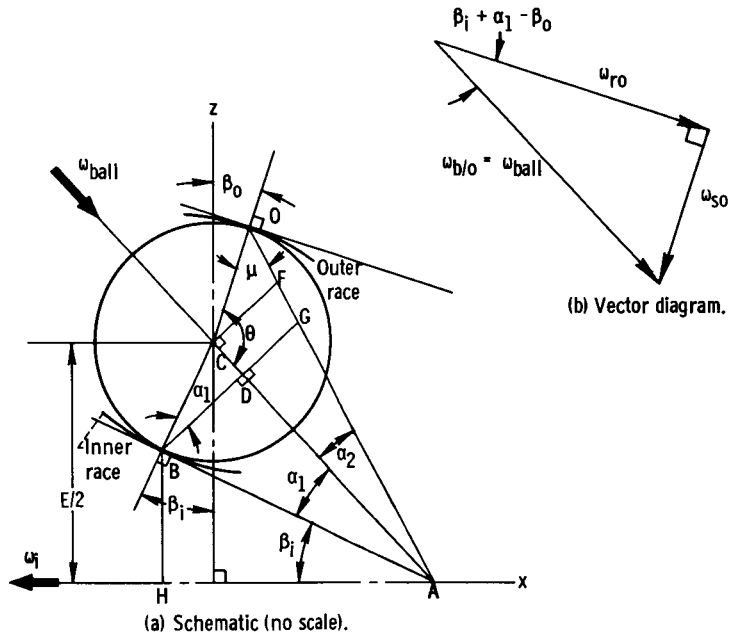

(b) Vector diagram.

(a) Schematic (no scale).

Figure 4. - Inner race control (ref. 8).

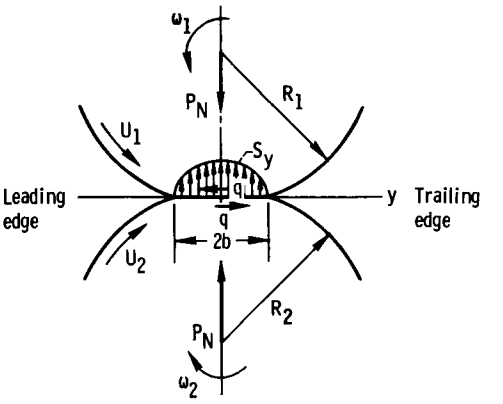

Figure 5. - Two cylinders of unit length under rolling contact (ref. 9).

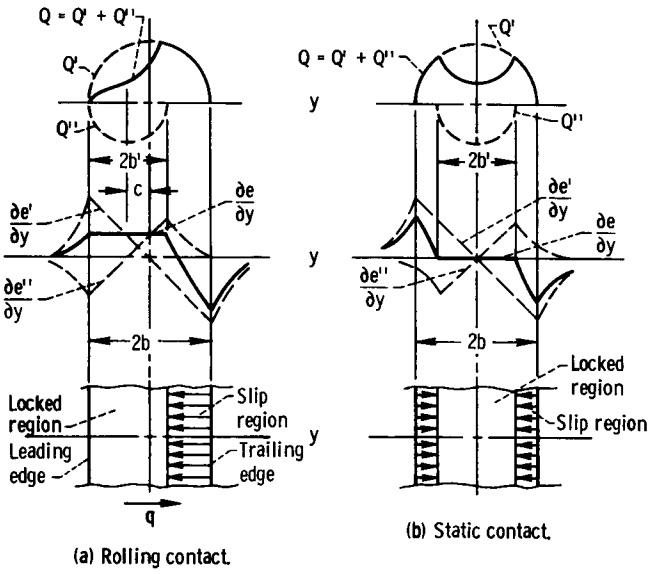

Figure 6. - Tangential tractions, surface strains, and micro-slip of two cylinders of unit length under rolling contact (ref. 9).

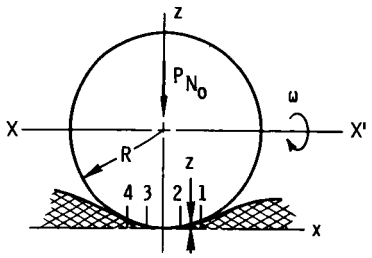

(a) Ball rolling on groove.

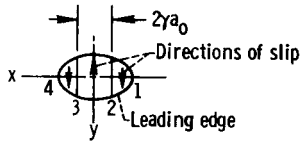

(b) Contact ellipse.

Figure 7. - Differential slip due to curvature of contact ellipse.

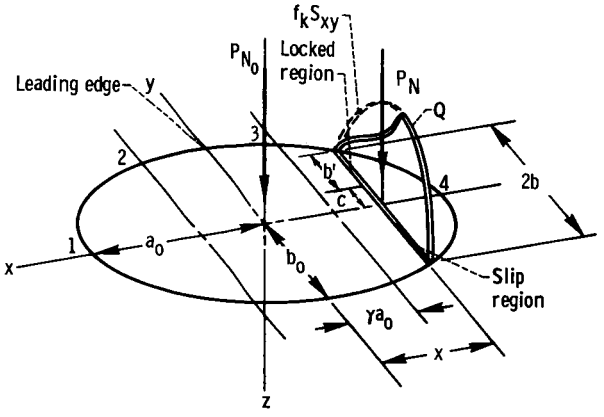

Figure 8. - Tangential tractions on an elemental strip of an elliptical contact area for a ball rolling freely in a conforming groove (ref. 9).

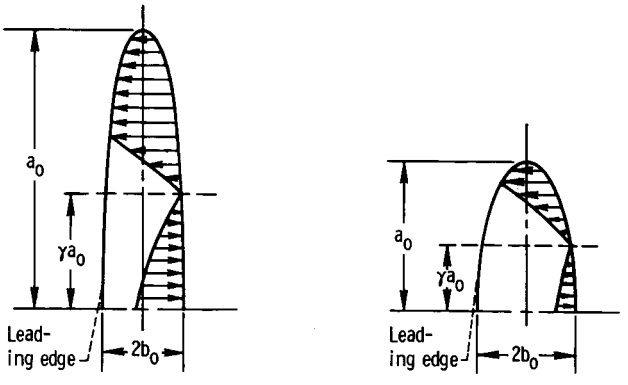

(a) Case a. (b) Case b.

Figure 9. - Microslip on the contact area of a ball rolling freely in a conforming groove (ref. 9).